Polarized parton distributions and Light-Front Dynamics

Pietro Faccioli[a,*], Marco Traini[a,†], and Vicente Vento[b,‡]

[a] *Dipartimento di Fisica, Università degli Studi di Trento,*

and Istituto Nazionale di Fisica Nucleare, G.C. Trento

I-38050 POVO (Trento), Italy

[b] *Departament de Física Teòrica, Universitat de València*

and Institut de Física Corpuscular, Centre Mixt Universitat de València,

Consejo Superior de Investigaciones Científicas,

E-46100 Burjassot (València) Spain

Abstract

We present a consistent calculation of the structure functions within a light-front constituent quark model of the nucleon. Relativistic effects and the relevance of the covariance constraints are analyzed for both polarized and unpolarized parton distributions. Various models, which differ in their gluonic structure at the hadronic scale, are investigated. The results of the full covariant calculation are compared with those of a non-relativistic approximation to show the structure and magnitude of the differences.

---

*present address: ECT⋆, Villa Tambosi, 38050 Villazzano, (Trento), Italy

†traini@science.unitn.it

‡vicente.vento@uv.es

I. INTRODUCTION

Constituent quark models, on one side, and the parton picture, on the other side, represent two complementary descriptions of hadron structure [1]. The rest frame (or laboratory) description, based on constituent quarks, and the infinite momentum frame description (P_∞), based on partons, appeared as formalisms capable of interpreting particle physics phenomena at different resolution scales. The algebraic approach, we are going to explore, seemed useful in establishing links between them [2]. It was intensively investigated in the late sixties, but a quantitative scheme for interacting scenarios was never attained.

The birth of the Quantum Chromodynamics (QCD) set the general framework to understand deep inelastic phenomena beyond the parton model. The perturbative approach to QCD is able to connect observables at different resolution scales, but the realization of the complete project, i.e., to fully understand the consequences of the dynamics of quarks and gluons, requires the input of unknown non-perturbative matrix elements to provide absolute values for the observables at any scale.

In the recent past the work by Glück, Reya and coworkers [3] has shown that, starting from a parton parametrization at a low resolution scale μ_0^2, the experimental deep inelastic structure functions at high momentum transfer can be reproduced and even predicted [4]. μ_0^2 is evaluated by evolving back the second moment of the valence distribution to the point where it becomes dominant. The procedure, suggested by Parisi and Petronzio [5], assumes that there exist a scale, μ_0^2, where the short range (perturbative) part of the interaction is negligible, therefore the glue and sea are suppressed, and the long range (confining) part of the interaction produces a proton composed of three (valence) quarks only. Jaffe and Ross [6] proposed thereafter, to adscribe the quark model calculations of matrix elements to that, hadronic scale, μ_0^2. For larger Q^2 their Wilson coefficients will give the evolution as dictated by perturbative QCD. In this way quark models, summarizing a great deal of hadronic properties, may substitute for low-energy parametrizations.

Following such a path, a partonic description can be generated from gluon radiation even

off a purely valence quark system, which can be used to generate the non perturbative input occurring in the Operator Product Expansion (OPE) analysis of lepton-hadron scattering in QCD [7]. A systematic analysis based on non-relativistic potential models, shows that the approach can be consistently developed at Next-to-Leading Order both for polarized and unpolarized structure functions [8], including non-perturbative contributions from the nucleon cloud [9] or from the partonic substructure of the constituent quarks [10]. The formulation of this naive approach has been motivated by simplicity and by the success of the constituent models in reproducing many properties of the hadronic spectrum in the 1 - 2 GeV region.

It has been quite evident, since the original formulation of many of these models, that relativistic effects to the nucleon wave function, as well as, covariance requirements, are needed even for a phenomenological description of the structure of hadrons. The present paper is devoted to the study of a possible generalization of our approach in that direction, and we will show that relativistic covariance can be incorporated within the same framework in a rather transparent and elegant manner. To this aim we develop a constituent quark model in the light-front realization of the Hamiltonian dynamics and apply to it the formalism for the calculation of both polarized and unpolarized parton distributions.

In the next section we proceed to reformulate the procedure using the Hamiltonian formalism in the light front dynamics. A light-front constituent quark model is defined and its momentum distributions are related to the quark distribution function at the hadronic scale in the conventional way. The third section is dedicated to analyze, under different hadronic conditions, the perturbative evolution required to reach the scale of the data. Two scenarios, characterized by the presence or absence of soft gluons at the hadronic scale, are studied. We end by summarizing our results and discussing those points, which at the light of our presentation, require further development.

II. QUARKS AND PARTONS

A schematic phenomenological distinction between constituent quarks and partons is often made by differentiating the infinite momentum frame, where partons show up, from the laboratory rest frame, where the constituent quarks appear to be the relevant degrees of freedom responsible for the correct symmetries and quantum numbers. Of course such a schematic point of view is only approximate and can also be at the origin of some misunderstanding. Actually the two descriptions appear well defined in the light-front description of deep inelastic scattering, where the parton model is recovered, in the Bjorken limit, due to the dominance of short light-cone distances ($z^2 \sim 0$) in the relevant Feynmann diagrams. As a consequence the partonic description can be developed in the rest frame of the hadron by using light-cone formalism. In particular the i-th parton distribution can be related to the light-cone momentum density[1].

$$q_i^{\uparrow (\downarrow)}(x, \mu_0^2) = \frac{1}{(1-x)^2} \int d^3k \; n_i^{\uparrow (\downarrow)}(\mathbf{k}^2) \, \delta \left(\frac{x}{1-x} - \frac{k^+}{M_N} \right) \; , \tag{1}$$

where $k^+/P^+ = k^+/M_N = (\sqrt{\mathbf{k}^2 + m_i^2} + k_z)/M_N$ is the light-cone momentum fraction of the struck parton in the rest frame, M_N and m_i are the nucleon and parton mass respectively and $n_i^{\uparrow}(\mathbf{k}^2)$, $n_i^{\downarrow}(\mathbf{k}^2)$ represent the light-cone density momentum density of the i-th parton whose spin is *aligned* ($\uparrow$) or *anti-aligned* ($\downarrow$) to the total spin of the parent nucleon. If one assumes that at the scale μ_0^2 only the u and d constituent quarks are resolved, the momentum densities can be written

$$n_{u(d)}^{\uparrow (\downarrow)}(\mathbf{k}^2) = \langle N, J_z = +1/2| \sum_{i=1}^{3} \frac{1 + (-)\tau_i^z}{2} \frac{1 + (-)\sigma_i^z}{2} \, \delta(\mathbf{k} - \mathbf{k}_i)|N, J_z = +1/2 \rangle \; . \tag{2}$$

The light-cone distributions (2) have been evaluated in the past making use of non-relativistic constituent quark models, while in the present investigation we want to improve their description including relativistic effects as introduced by a light-front formulation of a three-body

---

[1]A formal derivation of Eq. (1) can be found in ref. [8]. Eq. (1) includes the support correction as discussed in the same reference.

interacting system. As a consequence we will remain within a constituent picture where the partons in the rest frame are identified with three (constituent) quarks at the hadronic scale, and covariance requirement is fulfilled.

Since the hadronic scale μ_0^2 turns out to be very low ($\mu_0^2 \sim (0.1 - 0.2)$ GeV^2), close to the constituent quark mass[2], we assume that the constituent picture at this scale has to be identified with a Constituent Quark Model, whose parameters are fixed to reproduce the basic features of the nucleon spectrum in the energy region $1 - 2$ GeV.

A. The Light-Front Constituent Quark Model

Before discussing the details of the quark wave functions, it is worth to remark the main features of the theoretical framework that we have employed to achieve a covariant description of the nucleon's constituent degrees of freedom. An exhaustive review of covariant hamiltonian dynamics can be found in [11].

On a quantum level, the covariance requirement is formulated by demanding the probability assigned to a given event to be the same in all inertial frames. According to Wigner theorem [12], this is achieved if (and only if) the correspondence between the states in different frames is realized by means of an unitary representation $U(\Lambda, a)$ of the Poincaré group.

The connected component of the Poincaré group is a ten parameter Lie Group that includes four space time translations, three rotations and three Lorentz boosts. Let us denote with P^μ the representations of the generators of space-time translations, with K^j those of Lorentz boosts, and with J^j those of $SU(2)$. Any linear combination of generators is still a generator. To achieve a covariant formulation of the Poincaré Algebra it is convenient to introduce a new set of tensor generators of the Lorentz group:

---

[2]The actual value of the scale μ_0^2 ranges from 0.094 GeV^2, if only valence quarks are considered, to 0.37 GeV^2 [9], when non-perturbative $q - \bar{q}$ pairs and gluons are included.

$$J^{0j} = K^j \tag{3}$$

$$J^{jk} = \epsilon^{jkl} J_l \tag{4}$$

$$J^{\alpha\beta} = -J^{\beta\alpha}. \tag{5}$$

The tensor character of these operators is expressed by the following relationships:

$$U^\dagger(\Lambda) P^\mu U(\Lambda) = \Lambda^\mu_\nu P^\nu \tag{6}$$

$$U^\dagger(\Lambda) J^{\mu\nu} U(\Lambda) = \Lambda^\mu_\rho \Lambda^\nu_\sigma J^{\rho\sigma}. \tag{7}$$

Starting from the equations (6) and (7) it is possible to work out the following Algebra :

$$[P^\mu, P^\nu] = 0, \tag{8}$$

$$[J^{\mu\rho}, P^\nu] = i(g^{\mu\nu} P^\rho - g^{\rho\nu} P^\mu), \tag{9}$$

$$[J^{\mu\nu}, J^{\rho\sigma}] = i(g^{\mu\sigma} J^{\nu\rho} - g^{\mu\rho} J^{\nu\sigma} - g^{\nu\sigma} J^{\mu\rho} + g^{\nu\rho} J^{\mu\sigma}). \tag{10}$$

Hence, in order to build a covariant quantum mechanical model, one has to construct a model Hilbert space and find a set of operators such that these commutation relations are satisfied.

In general, such a representation is not unique and depends on the interaction. However, it is possible to single out a subset of generators which do not contain the interaction. Such operators group together to form the *kinetic subgroup*. Once the kinetic subgroup is determined, the whole set of generators is also fixed including the *Hamiltonian* generators (i.e. those operators which contain the interaction). Dirac proposed [13] to fix first the kinetic subgroup identified with the stability group of a three-dimensional surface in Minkowski's space, and then extract the Hamiltonian generators by group representation properties.

The choice of the surface that determines the kinetic subgroup fixes the *form of the dynamics*. In the following we will use the light-front form of the dynamics whose invariant surface is the light-front (null) plane $x^0 + x^3 = 0$. This form of the dynamics has many important properties, for example, it leads to the largest possible kinetic subgroup.

In the light-front form of the dynamics, it is convenient to consider the following set of generators: P^1, P^2, $P^+ = P^0 + P^3$, J^3, K^3 (kinetic subgroup) and $P^- = P^0 - P^3$, $\mathbf{F}_\perp = \mathbf{K}_\perp + \hat{\mathbf{z}} \times \mathbf{J}_\perp$ (set of Hamiltonians). In particular, the role of the Hamiltonian H of non relativistic Quantum Mechanics is played, in the front form, by the generator P^- of translations along the direction orthogonal to the null plane. This operator has a positive eigenvalued spectrum and this prevents the existence of negative "energy" states, allowing for the number of particles to be fixed. For this reason the light-front form of the dynamics is particularly well suited to describe a low energy model where only three valence quarks are considered.

The construction of a representation of the Poincaré space such that the kinetic subgroup is the stability group on the light-front, is clearly much easier by using a parametrization of the Minkowski space which is as close as possible to the symmetry of the problem, i.e. the light-front coordinates: $x^+ = x^0 + x^3$, $x^- = x^0 - x^3$, x^1 and x^2. In this way a vector is given by $(x^+, x^-, x^1, x^2) = (x^+, x^-, \mathbf{x}_\perp)$, an the scalar product by $x \cdot y = -\frac{1}{2}x^+y^- - \frac{1}{2}x^-y^+ + \mathbf{x}_\perp \cdot \mathbf{y}_\perp$. The null plane is the plane with $x^+ = 0$ and the "(three)-vector" $(x^-, \mathbf{x}_\perp)$ on that plane is a true three-vector under light-front boosts (i.e. the boost belonging to the kinetic subgroup).

In order to model the Hilbert space one needs to combine the generators of the Poincaré group to get a set of self commuting operators which have a physical interpretation. By combining P^μ, $J^{\mu\nu}$ one can construct two invariants:

i) the mass operator

$$M^2 = -P^2 = P^+P^- - \mathbf{P}_\perp^2 ,$$

ii) and the square $(W_\mu W^\mu)$ of the *Pauli-Lubansky* vector:

$$W_\mu = \frac{1}{2} P^\nu J^{\rho\sigma} \epsilon_{\nu\rho\sigma\mu} .$$

In relativistic systems the definition of the spin operator is related to the Pauli-Lubansky vector: one defines, in fact, the square of the spin by

$$W^2 = -M^2 j^2. \tag{11}$$

It can be proved that there is an infinite set of operator-valued vectors satisfying the relation (11). Therefore, the spin operator is defined as a linear combination of W_μ and M^{-1}:

$$j_\alpha = u_\alpha^\mu(P) W_\mu M^{-1} . \tag{12}$$

The coefficients $u_\alpha^\mu(P)$ are space-like operator-valued vectors of an orthonormal basis [14]. Different choices of this basis leads to the specific definition of spin in different forms of the dynamics. Starting from (12) one can prove that the spin operator transforms as

$$U^\dagger(\Lambda) \, \vec{j} \, U(\Lambda) = R_W(\Lambda, P) \, \vec{j}, \tag{13}$$

where $R_W(\Lambda, P)_{\alpha\beta} = U_\alpha(\Lambda P) \cdot \Lambda \, u_\beta(P)$ is called Wigner rotation. One can demonstrate that defining $u_0(P) = P/M$, the 16 components quantity $u_\mu^\nu(P)$ forms a $SO(1,3)$ representation of a Lorentz transformation. The spin operator can be written

$$j_\alpha = \frac{1}{2} \, \epsilon_{0\alpha\beta\gamma} \, u_\rho^\beta(P) \, u_\sigma^\gamma(P) \, J^{\rho\sigma} = \frac{1}{2} \epsilon_{0\alpha\beta\gamma} u_\rho^\beta(P) \, u_\sigma^\gamma(P) \sum_i^n J_i^{\rho\sigma} , \tag{14}$$

where the last equality holds when the system is made up of n independent constituents. In the *instant form* of the dynamics (in which the invariant surface is chosen to be the equal-time plane) the Wigner transformations associated to a rotation is the rotation itself and the spin is called *canonical*. One can demonstrate that, in this form of the dynamics, the ordinary composition rules of the angular momentum hold, providing one rotates the constituent spins by means of appropriate Wigner rotations. In the case of light-front form of the dynamics, the Wigner rotations associated to a light-front boosts are the identity. The ordinary composition laws for the total angular momentum hold, provided we transform the light-front spin into the canonical spin. The transformation that relates the light front spin to the canonical spin is called a Melosh rotation,

$$R_M(P)_{\alpha\beta} := u_\alpha^\mu(P)^{can.} u_\beta^\nu(P)^{l.f.} g_{\mu\nu} \tag{15}$$

Its spin-$\frac{1}{2}$ representation is:

$$D^{\frac{1}{2}}[R_M(\mathbf{P}, M)] = \frac{M + P^+ - i\vec{\sigma} \cdot (\hat{z} \times \mathbf{P}_\perp)}{\sqrt{(M + P^+)^2 + \mathbf{P}_\perp^2}} . \tag{16}$$

8

1. Non-interacting and interacting systems on the light-front

The single spin-1/2 particle states can be described by wave functions $\phi(\tilde{p}, \lambda)$, where $\tilde{p} = (p^+, \mathbf{p}_\perp)$ is the momentum three-vector on the light-front and λ the longitudinal spin component. One has:

$$||\phi||^2 = \sum_{\lambda=-j}^{\lambda=+j} \int \frac{d^3[\tilde{p}]}{p^+} |\phi(p^+, \mathbf{p}_\perp)|^2 \,,$$

$$d^3[\tilde{p}] = dp^+ \, d^2\mathbf{p}_\perp \, \theta(p^+) \,; \tag{17}$$

where the measure $d^3[\tilde{p}]/p^+$ and the component λ are invariant under the kinematic transformations, and the factor $1/\sqrt{p^+}$ can be included in the definition of the wave function provided we change its light-front boost transformation properties accordingly.

For a many-body system of n non-interacting particles the wave function can be written $\Phi(\tilde{p}_1, \lambda_1; ...; \tilde{p}_n, \lambda_n)$, and Eq. (17) becomes

$$||\Phi||^2 = \sum_{\lambda_1,...,\lambda_n} \int \left(\prod_{i=1}^{n} \frac{d^3[\tilde{p}_i]}{p_i^+} \right) |\Phi(\tilde{p}_1, \lambda_1; ...; \tilde{p}_n, \lambda_n)|^2 \,. \tag{18}$$

Quite often it is more useful to represent Φ as functions of the total momentum on the light-front $\tilde{P} = \sum_{i=1}^{n} \tilde{p}_i$, the momentum fraction $x_i = p_i^+/P^+$, and the transverse relative momenta $\mathbf{k}_{i\perp} = u_\perp \cdot p_i = \mathbf{p}_{i\perp} - x_i \mathbf{P}_\perp$. Eq. (18) can be then transformed into

$$||\Phi||^2 = \sum_{\lambda_1,...,\lambda_n} \int \frac{d^3[\tilde{P}]}{P^+} \int \left(\prod_{i=1}^{n} \frac{dx_i}{x_i} d^2\mathbf{k}_{i\perp} \right) \delta \left(\sum_{i=1}^{n} x_i - 1 \right) \delta \left(\sum_{i=1}^{n} \mathbf{k}_{i\perp} \right) \times$$

$$\times \, |\Phi(\tilde{P}, \mathbf{k}_{1\perp}, x_1, \lambda_1; ...; \mathbf{k}_{n\perp}, x_n, \lambda_n)|^2 \,. \tag{19}$$

One can introduce a further set of coordinates adding, on kinematical basis only, a third component k_{i3} to the transverse momenta $\mathbf{k}_{i\perp}$ boosting the lab momenta p_i:

$$k_{i3} = u_3(P) \cdot p_i = \frac{1}{2} \left[M_0 x_i + \frac{m_i^2 + \mathbf{k}_{i\perp}^2}{M_0 x_i} \right] = M_0 x_i - \omega_i \,,$$

$$\omega_i = -u_0(P) \cdot p_i = \frac{1}{2} \left[M_0 x_i - \frac{m_i^2 + \mathbf{k}_{i\perp}^2}{M_0 x_i} \right] \,, \tag{20}$$

where the total mass operator of the system

$$M_0 = \sum_i \sqrt{\mathbf{p}_i^2 + m_i^2} = \sqrt{\sum_i \frac{\mathbf{k}_{i\perp}^2 + m_i^2}{x_i}} = \sum_i \omega_i = \sum_i \sqrt{\mathbf{k}_i^2 + m_i^2} \ . \tag{21}$$

The invariant measure to be used in the definition of the scalar product transforms in the following way:

$$\left(\prod_{i=1}^n \frac{dx_i}{x_i} d^2\mathbf{k}_{i\perp} \right) \delta \left(\sum_{i=1}^n x_i - 1 \right) \delta \left(\sum_{i=1}^n \mathbf{k}_{i\perp} \right) \to \left(\prod_{i=1}^n \frac{d^3\mathbf{k}_i}{\omega_i} \right) M_0 \, \delta \left(\sum_{i=1}^n \mathbf{k}_i \right) \ . \tag{22}$$

The total spin, in the new coordinate system, is

$$\vec{j} = \sum_{l=1}^n \left[i \vec{\nabla}_{\mathbf{k}_l} \times \mathbf{k}_l + \vec{s}_l \right] \ , \tag{23}$$

with

$$\vec{s}_l = R_M(\mathbf{k}_l, m_l) \, \vec{j}_l \tag{24}$$

and the representation of the Melosh rotation reads

$$D^{\frac{1}{2}} \left[R_M(\mathbf{k}_i, m_i) \right] = \frac{m_i + x_i M_0 - i\vec{\sigma} \cdot (\hat{z} \times \mathbf{k}_{i\perp})}{\sqrt{(m_i + x_i M_0)^2 + \mathbf{k}_{i\perp}^2}} \ . \tag{25}$$

As a first consequence of this section we can conclude that the dynamics of n non-interacting spin $1/2$ particles can be described, on the light-front, by a wave function $\psi(\tilde{P}, \mathbf{k}_1, \mu_1; ...; \mathbf{k}_n, \mu_n)$ whose norm is given by

$$||\psi||^2 = \langle \psi | \psi \rangle = \sum_{\mu_1, ..., \mu_n} \int \frac{d^3\tilde{P}}{P^+} \left(\prod_{i=1}^n d^3\mathbf{k}_i \right) \delta \left(\sum_{i=1}^n \mathbf{k}_i \right) |\psi|^2 \ , \tag{26}$$

where μ_i are the eigenvalues of the spin projections s_i^z of eq.(24). We stress that the Jacobian and the invariant measure of the transformation $(\mathbf{k}_{i\perp}, x_i) \to \mathbf{k}_i$, has been absorbed in the definition of the wave functions ψ as can be seen from Eq. (26) (cfr. the discussion after Eq. (17)).

The extension to interacting systems requires a dynamical representation of the Poincarè group. One way to achieve this is to add an interaction V to the free mass operator M_0

$$M = M_0 + V \ , \tag{27}$$

where V is the interaction. All the other definitions remain unaffected, including the definition of the third component of the relative momenta k_{i3}, because the boosts we use are interaction independent. All required commutation relations are satisfied if the mass operator commutes with the total spin $\vec{j}$ and with the kinematic generators. In the representation in which states are represented by functions of $\tilde{P}$, $\mathbf{k}_i$ and μ_i these conditions are realized if:

i) V is independent on the total momentum $\tilde{\mathbf{P}}$;

ii)V is invariant under ordinary rotations.

Summarizing: in the light-front formulation of the quark dynamics, the intrinsic momenta of the constituent quarks (k_i) can be obtained from the corresponding momenta (p_i) in a generic reference frame through a light-front boost $(k_i = u(P) \cdot p_i, \ P \equiv \sum_{i=1}^{3} p_i)$ such that the Wigner rotations reduce to the identity. The spin and spatial degrees of freedom are described by the wave function:

$$\Psi = \frac{1}{\sqrt{P^+}} \, \delta(\tilde{P} - \tilde{p}) \, \chi(\mathbf{k}_1, \mu_1, \ldots, \mathbf{k}_3, \mu_3), \tag{28}$$

where μ_i refer to the eigenvalue of the light-front spin, so that the spin part of the wave function is transformed by the tensor product of three independent Melosh rotations: $R_{\mathrm{M}}^{\dagger}(\mathbf{k}_i, m_i)$ [2], namely $\mathcal{R}^{\dagger} = \prod_{\otimes, i=1}^{3} R_{\mathrm{M}}^{\dagger}(\mathbf{k}_i, m_i)$.

The internal wave function is an eigenstate of the baryon mass operator $M = M_0 + V$, with $M_0 = \sum_{i=1}^{3} \omega_i = \sum_{i=1}^{3} \sqrt{\mathbf{k}_i^2 + m_i^2}$, where the interaction term V must be independent on the total momentum $\tilde{P}$ and invariant under rotations.

The nucleon state is then characterized by isospin (and its third component), parity, light-front (non-interacting) angular momentum operators J and projection J_n, where the unitary vector $\hat{n} = (0, 0, 1)$ defines the spin quantization axis.

B. Valence Quark Hamiltonian

In the present work we will discuss results of a confining mass equation (27) of the following kind

$$(M_0 + V)\,\psi_{0,0}(\xi) \equiv \left(\sum_{i=1}^{3} \sqrt{\mathbf{k}_i^2 + m_i^2} - \frac{\tau}{\xi} + \kappa_l\,\xi\right) \psi_{0,0}(\xi) = M\,\psi_{0,0}(\xi)\,, \tag{29}$$

where $\sum_i \mathbf{k}_i = 0$, $\xi = \sqrt{\vec{\rho}^{\,2} + \vec{\lambda}^{\,2}}$ is the radius of the hyper-sphere in six dimension and $\vec{\rho}$ and $\vec{\lambda}$ are the intrinsic Jacobi coordinates $\vec{\rho} = (\mathbf{r}_1 - \mathbf{r}_2)/\sqrt{2}$, $\vec{\lambda} = (\mathbf{r}_1 + \mathbf{r}_2 - 2\,\mathbf{r}_3)/\sqrt{6}$. The choice of the mass operator (29) has a twofold motivation:

i) Simplicity. This is a first attempt to develop a covariant approach to DIS based on quark models, therefore we use a mass operator whose symmetry properties facilitate the numerical solutions. In this respect the choice of a hypercentral potential has big advantages.

ii) The nucleon spectrum is reproduced. This has been demonstrated both within non-relativistic [15] and relativistic [16] approaches [3]. In particular the well known problem of the mass of the Roper is solved in the present case by the use of τ/ξ potential, as discussed by Ferraris et al. [15]. Of course our aim is much less ambitious than reproducing all the complexity of the baryon spectrum, we restrict the calculation to the nucleon wave function and we do not consider spin-dependent terms assuming pure $SU(6)$-symmetric states[4].

The intrinsic nucleon state is antisymmetric in the color degrees of freedom and symmetric with respect the orbital, spin and flavor coordinates. In particular, disregarding the color part, one can write

---

[3] In ref. [16] a simplified version of the same mass operator has been introduced to investigate the baryonic mass spectrum in the instant form dynamics. Namely the eigenstates of the operator $\hat{M}^2 = \sum_i (\mathbf{k}_i^2 + m_i^2) - a/\xi + b\xi$ are discussed, and the potential $-a/\xi + b\xi$ is the simplified form of the more complex expression $V^2 + \{M_0, V\} + \sum_{i\neq j} \sqrt{\mathbf{k}_i^2 + m_i^2}\,\sqrt{\mathbf{k}_j^2 + m_j^2}$ obtained by squaring the correct mass operator $\hat{M} = M_0 + V$. We will discuss solutions of the mass operator Eq. (29) directly, without further simplification.

[4] Adding a perturbative hyperfine interaction as discussed in ref. [15] in the context of non-relativistic Hamiltonians, would be rather simple also within the relativized scheme of Eq. (29). At the present stage we neglect such a complication, but a more complete study of the nucleon spectrum should include $SU(6)$-breaking terms within the light-front approach.

$$|N, J, J_n = +1/2\rangle = \psi_{0,0}(\xi)\, \mathcal{Y}_{[0,0,0]}^{(0,0)}(\Omega)\, \frac{\chi_{MS}\phi_{MS} + \chi_{MA}\phi_{MA}}{\sqrt{2}} \,, \qquad (30)$$

where $\psi_{\gamma,\nu}(\xi)$ is the hyper-radial wave function solution of Eq. (29), $\mathcal{Y}_{[\gamma,l_\rho,l_\lambda]}^{(L,M)}(\Omega)$ the hyper-spherical harmonics defined in the hyper-sphere of unitary radius, and ϕ and χ the flavor and spin wave function of mixed $SU(2)$ symmetry. Let us note that, in order to preserve relativistic covariance, the spin wave functions

$$\chi_{MS} = \frac{1}{\sqrt{6}}\, [2 \uparrow\uparrow\downarrow - (\uparrow\downarrow + \downarrow\uparrow)\uparrow] \,; \qquad \chi_{MA} = \frac{1}{\sqrt{2}}\, (\uparrow\downarrow - \downarrow\uparrow)\uparrow \,, \qquad (31)$$

have to be formulated by means of the appropriate Melosh transformation of the i-*th* quark spin wave function:

$$\uparrow_i \equiv\ R_{\mathrm{M}}(\mathbf{k}_i, m_i) \begin{pmatrix} 1 \\ 0 \end{pmatrix} = \frac{1}{\sqrt{(m_i + x_i M_0)^2 + \mathbf{k}_{i\perp}^2}} \begin{pmatrix} m_i + x_i M_0 \\ k_{iR} \end{pmatrix} \qquad (32)$$

$$\downarrow_i \equiv\ R_{\mathrm{M}}(\mathbf{k}_i, m_i) \begin{pmatrix} 0 \\ 1 \end{pmatrix} = \frac{1}{\sqrt{(m_i + x_i M_0)^2 + \mathbf{k}_{i\perp}^2}} \begin{pmatrix} -k_{iL} \\ m_i + x_i M_0 \end{pmatrix} \qquad (33)$$

where $x_i = p_i^+/P^+ = (k_{iz} + \omega_i)/M_0$ and $k_{L/R} = k_x \pm i\, k_y$.

1. Numerical Solutions

We have solved the mass equation (29) numerically by expanding the hyper-radial wave functions $\psi_{\gamma\nu}(\xi)$ on a truncated set of hyper-harmonic oscillator basis states. The matrix elements of the mass operator (29) have been calculated in momentum space for the kinetic energy term, and in configuration space for the interaction one. Making use of the Rayleigh-Ritz variational principle the HO constant has been determined and convergence has been reached considering a basis as large as 17 HO components [17]. The parameters of the interaction, have been determined phenomenologically in order to reproduce the basic features of the (non strange) baryonic spectrum up to ≈ 1500 MeV, namely the position of the Roper resonance and the average value of the 1^- states. We obtain: $\tau = 3.3$ and $\kappa_l = 1.8$

fm^{-2} [17] to be compared with the corresponding non-relativistic fit $\tau = 4.59$ and $\kappa_l = 1.61$ fm^{-2} [15]. The constituent quark masses have been chosen $m_u = m_d = m_q = M_N/3$.

The result of this reparametrization is that a huge amount of high momentum components is generated by solving the mass equation (cfr.Fig. 1a), and they play an important role in the evaluation of transition and elastic form factors within light-front constituent quark models as discussed by Caldarelli et $al.$ [18] in connection with the solutions of the Isgur-Capstick model Hamiltonian. From the point of view of DIS the enhancement of high momentum components in the density distribution of the valence quarks is crucial to reproduce the behavior of the unpolarized structure functions for large value of the Bjorken variable x as it will be discussed in the next section where also polarized responses are investigated at the hadronic scale.

C. Partons at the Hadronic Scale

The calculation of the partonic content at the hadronic scale as given by Eq. (1), is rather involved mainly because of the spin dynamics accounted for by the Melosh rotations (32) and (33), but finally the polarized distributions at the hadronic scale can be written in a rather elegant way:

$$\mathcal{Q}(x, \mu_0^2) = \frac{\pi}{9} \frac{M_N}{(1-x)^2} \int_0^\infty dt \, n(\tilde{k}_z^2, t) \frac{a_\mathcal{Q} \left(m + \sqrt{\tilde{k}_z^2 + t + m^2} + \tilde{k}_z \right)^2 + b_\mathcal{Q} \, t}{\left(m + \sqrt{\tilde{k}_z^2 + t + m^2} \right)^2 + t} D(\tilde{k}_z, t) \quad (34)$$

where $\mathcal{Q} \equiv u^{\uparrow \, (\downarrow)}, d^{\uparrow \, (\downarrow)}$, $t \equiv \mathbf{k}_\perp^2$,

$$D(\tilde{k}_z, t) = \frac{\sqrt{t + \tilde{k}_z^2 + m^2}}{\left| \sqrt{t + \tilde{k}_z^2 + m^2} + \tilde{k}_z \right|} \quad , \quad (35)$$

$$\tilde{k}_z(x, t) = \frac{M_N}{2} \left[\frac{x}{1-x} - \frac{(t + m^2)}{M_N^2} \frac{(1-x)}{x} \right] \quad ,$$

and $n(\tilde{k}_z^2, \mathbf{k}_\perp^2)$ is the total momentum density distribution of the valence quarks in the nucleon calculated making use of the eigenfunction ψ_{00} of Eq. (29):

14

$$n(\mathbf{k}^2) = 3 \int |\psi_{0\,0}|^2 \, \delta(\mathbf{k} - \mathbf{k}_3) \, \delta(\sum_i \mathbf{k}_i) \, d^3\mathbf{k}_1 d^3\mathbf{k}_2 d^3\mathbf{k}_3 \ , \tag{36}$$

with $\int d^3\mathbf{k} \, n(\mathbf{k}^2) = 3$. The coefficients $a_{\mathcal{Q}}$ and $b_{\mathcal{Q}}$ take the values $a_{u\uparrow} = b_{u\downarrow} = 5; \; b_{d\uparrow} = a_{d\downarrow} = 2;$ $b_{u\uparrow} = a_{u\downarrow} = a_{d\uparrow} = b_{d\downarrow} = 1.$

1. Effects of Melosh Rotations

The effects of high momentum components on the unpolarized parton distributions $\sum_{q=(u,d)} (q^\uparrow(x,\mu_0^2) + q^\downarrow(x,\mu_0^2)) = u_V(x,\mu_0^2) + d_V(x,\mu_0^2)$ at the hadronic scale are shown in Fig. 1b. Their important rôle in reproducing the correct behavior of the structure functions for large values of the Bjorken variable x will be discussed in the next sections. The relevant effects of relativistic covariance are even more evident looking at the polarized distributions $\Delta u_V(x,\mu_0^2) = u^\uparrow(x,\mu_0^2) - u^\downarrow(x,\mu_0^2)), \Delta d_V(x,\mu_0^2) = d^\uparrow(x,\mu_0^2) - d^\downarrow(x,\mu_0^2))$ where the spin dynamics on the light-front plays a crucial rôle. The introduction of the Melosh rotations results in a substantial enhancement of the responses at large x and in an suppresion of the response for $0.1 \lesssim x \lesssim 0.5$ as can be seen from Fig. 2. We show, in the same figure, also the predictions of a pure relativized solution obtained by solving numerically Eq. (29) and neglecting the Melosh rotation effects in (34). Such a calculation retains the contribution due to the high momentum components, while the covariance requirement on the parton distribution is lost. One can argue on the quite relevant rôle of covariance on the spin observables.

2. Non-perturbative Gluons

A natural choice for the unpolarized gluon distribution within the present approach, has been discussed in refs. [8] and assumes a *valence-like* form (cfr. also ref. [3])

$$G(x,\mu_0^2) = \frac{\mathcal{N}_g}{3} \left[u_V(x,\mu_0^2) + d_V(x,\mu_0^2) \right] \ . \tag{37}$$

This definition implies $\int G(x, \mu_0^2)\, dx = 2$ and therefore only 60% of the total momentum is carried by the valence quarks at the scale μ_0^2. In this case $\mu_0^2 = 0.220$ GeV^2 at NLO ($[\alpha_s(\mu_0^2)/(4\,\pi)]_{\rm NLO} = 0.053$).

If the gluons were fully polarized at the scale μ_0^2 one would have $|\Delta G(x, \mu_0^2)| = G(x, \mu_0^2)$. However recent next-to-leading (NLO) studies of polarized Deep Inelastic Scattering (DIS) [19–25] show that the x-shape of ΔG is hardly constrained by the present data. As a consequence quite a few sets of parton distributions, with rather different x-shapes of the gluon component, provide very good descriptions of the same data. In particular the sign of $\Delta G(x, Q^2)$ for $x \gtrsim 0.1$ is not convincingly fixed: in the parametrization C of ref. [21] it is assumed to be *negative*, while it is taken *positive* in other cases (cfr., for example, ref. [22]).

In the recent past different authors have discussed the *sign* of the gluon contribution to the nucleon's spin in the light-cone gauge ($A^+ = 0$) and at the hadronic scale valid at the quark model level. In particular Ball, Forte and Ridolfi [19] showed the compatibility of the experimental data with a large and *positive* gluon polarization at $Q^2 = 1$ GeV^2 ($\Delta G(Q^2) = \int_0^1 dx \Delta G(x, Q^2) \approx 1.6 \pm 0.9$); Jaffe [26] showed that the color electric and magnetic fields, which are believed to be responsible for the spin splittings among light baryons, give rise to a significant *negative* contribution ($\Delta G(\mu_0^2) \approx -0.7$) at the hadronic scale; Mankiewicz, Piller and Saalfeld [27] performed a QCD sum rule calculation obtaining $\Delta G(\mu_0^2) \approx 2.1 \pm 1.0$, while Barone, Calarco and Drago [28], by using the non-relativistic quark model of Isgur-Karl and considering the renormalization due to self-interaction contributions, obtained $\Delta G(\mu_0^2 = 0.25$ GeV$^2) \approx 0.24$.

We shall describe results in two scenarios characterized by different gluon distributions (ΔG) at the hadronic scale [8]:

i) Scenario A : $\Delta G(x, \mu_0^2) = 0$. Only quark valence distributions are allowed at the hadronic scale. The momentum sum rule determines $\mu_0^2 = 0.094$ GeV^2 at NLO ($[\alpha_s(\mu_0^2)/(4\,\pi)]_{\rm NLO} = 0.142$).

ii) Scenario B: $\Delta G(x, \mu_0^2) = f\, G(x, \mu_0^2)$. f is the fraction of polarized gluons and has to

16

be considered with the appropriate sign. For example the Jaffe's suggestion, in our approximation scheme, would imply $\Delta G(x, \mu_0^2) \approx -0.35\, G(x, \mu_0^2)$, while $f > 0$ will imply positively polarized gluons [5].

III. RESULTS

A. Partonic bremsstrahlung

An important aspect of our approach is that we perform, in both the flavor non-singlet and singlet channels, a complete analysis at Next-to-Leading Order, an essential requirement needed to include the anomalous (γ_5) contributions consistently. Complete NLO calculation of all polarized two-loop splitting functions [29], in the $\overline{MS}$ renormalization and various factorization schemes [24,25,29]), are now available. The evolution of the polarized distributions is performed according to the solution of the renormalization group equation inverting the moments $\langle f(Q^2) \rangle_n = \int_0^1 dx\, f(x, Q^2)\, x^{n-1}$ numerically. Since the starting point for the evolution (μ_0^2), consistent with the renormalization scale of the quark model, is rather low, the form of the equations must guarantee complete symmetry for the evolution from μ_0^2 to $Q^2 \gg \mu_0^2$ and *back* avoiding additional approximations associated with Taylor expansions and not with the genuine perturbative QCD expansion (a complete discussion on the evolution procedure can be found in ref. [8]).

We use the so called $\overline{MS}$ and AB factorization scheme evolutions on our model input to show that our results are largely independent of which one we use. In principle the calculation should be independent of factorization scheme, however at present it is not straightforward to abscribe the non-perturbative input to any specific factorization scheme. The spurious

---

[5]In fact in ref. [26] it has been shown that $\int \Delta G(x, \mu_0^2)\, dx < 0$. Such inequality does not imply $\Delta G(x, \mu_0^2) < 0$ in the whole x-range, and our results for positively and negatvely polarized gluons can be seen as upper and lower limits for both cases.

factorization dependence arises because we associate the same non-perturbative input to the different factorization schemes as discussed in the next sections.

B. Discussion

1. Polarized Parton Distributions

In Fig. 3 the results for the proton structure function $g_1^p(x, Q^2)$ are shown and compared with the experimental data. The non-relativistic approximation of the present calculation appears to reproduce rather poorly the experimental observations. Even the use of non-relativistic models which reproduce rather well the whole baryon spectrum does not alter this conclusion, as shown in ref. [8] where the predictions of quite a few non-relativistic models are discussed.

The full covariant calculation leads to a theoretical predictions quite close to experimental data in the region $0.01 \leq x \lesssim 0.4$ even within the simple assumption of a pure valence component at the hadronic scale (scenario A). The calculation is parameter-free and the only adjustable parameters of the Hamiltonian (τ and κ_l in Eq. (29)) have been fixed to reproduce the low-lying nucleon spectrum as discussed in section II B 1.

The effect of relativistic covariance in the quark wave function is mainly associated to the spin dynamics induced by the Melosh rotations (cfr. Eqs.(32), (33), (34)) and these transformations lead to a strong suppression of the structure function in the small-x region ($x \lesssim 0.5$).

In order to introduce the gluons non perturbatively we evolve the unpolarized distributions predicted by the scenario A, up to the scale of scenario B where 60% of the total momentum is carried by valence quarks. At that scale we add to the valence partons the non-perturbative gluons as defined in Eq. (37) of section II C 2.

Moreover, at the new hadronic scale, the fraction of polarized gluons is chosen to be *negative* according to Jaffe's result [26] or *positive* as in other parametrizations. Note that

by choosing a negative fraction we are maximizing the difference with respect to the radiative gluons, because those yield to a positive polarization. Fig. 6 leads us to confirm that the low-x data on g_1^p do not constrain the gluon polarization strongly. If we vary the fraction of polarized gluons from 35% to 100% the quality of the agreement is not significantly changed in the region $0.01 \leq x \lesssim 0.4$. For larger values of x the valence contribution plays a major role and the behavior of the structure functions might depend on the model wave functions.

For both scenarios the boundary value μ_0^2 is rather low and one could question on higher order contributions to the evolution. In order to appreciate (and maximize) the relevance of NNLO (or higher order) effects, the polarized proton structure function are evolved at $Q^2 = 3$ GeV^2 within the scenario A and by using both LO and NLO approximations (cfr. Fig. 4). In the region of $0.01 \lesssim x \lesssim 0.5$ they differ roughly of 20% which represents the order of magnitude of the largest higher leading effects. The same evolution obtained within the scenario B would lead to an even smaller difference ($\lesssim 10\%$) between LO and NLO results.

The comparison of the predicted neutron structure function with the data (Fig. 5) differs quite substantially according to the amount of polarized gluons at the hadronic scale. Within scenario A the values of $g_1^n(x, Q^2)$ remain quite small according to the fact that the mass operator chosen (29) is $SU(6)$ symmetric. The introduction of *negative* gluon polarization brings the predictions of the present relativistic quark model closer to the experimental observations at least in the $x \geq 0.1$ region; a larger *negative* fraction of gluon polarization is favored by the data as can be argued also from the results of *positively* polarized gluons as shown in the same figure. Any how, since the neutron structure function is largely dependent on the nucleon wave function model, our assumption on $SU(6)$ symmetry is the largest source of uncertainty and a more detailed study of g_1^n should include more complex wave function models. Another source of uncertainty in our evaluation of the neutron stucture function is the lack, at the hadronic scale, of (polarized) sea contributions which can play even a major rôle for $x \lesssim 0.3$ [10].

All these limitations, however, do not obscure the main aim of our study, namely the discussion on the effects due the relativistic requirement of the quark wave function.

Fig. 6 is devoted to the gluon distributions. Within scenario A the polarized gluon distributions remain *positive* at the experimental scale as a result of the NLO evolution. On the contrary a large amount of *negative* gluon polarization is predicted within scenario B if one assumes anti-aligned gluons at the hadronic scale. The distribution is largely dependent on the polarization fraction. The dotted line of Fig. 6a shows the consequence, in the deep inelastic regime, of the Jaffe's calculation at low energy. The absence of non-perturbative sea polarization results in a huge (and probably unrealistic) amount of negative gluon polarization to reproduce the neutron data. Such a large amount of gluons is, however, inconsistent with the unpolarized gluon distributions as it is shown in Fig. 6b (dotted line again).

Fig. 7 shows the results of the analysis on the factorization scheme dependence. We have chosen to show both the proton and the more appreciable case of the polarized neutron data. The small difference gives us confidence in the results.

<center>*2. Unpolarized parton distributions*</center>

Figs. 8 and 9 complete our study of unpolarized partons (gluons are shown in Fig. 6 as already mentioned). Particularly evident is the improvement, due to the high momentum components introduced by the relativized solution, in describing the proton F_2 distribution in the region $0.4 \lesssim x \lesssim 0.8$. The non-relativistic description is largely suppressed for $x > 0.4$ due to the lack of high momentum contributions. The solution of the mass operator (29) have the appropriate components to contribute in this x-region . The work is completed by the comparison of LO NLO evolution also in the case of unpolarized scattering (Fig. 8a) and the results on valence and sea distributions (Fig. 9). In this last case one could repeat the comments already formulated for the polarized distributions: the lack of non-perturbative sea at the hadronic scale largely limits the possibility of reproducing the parton distributions in the singlet sector.

<center>20</center>

IV. FURTHER DEVELOPMENTS AND CONCLUSIONS

The present paper is devoted to a semi-quantitative analysis of the effects due to relativistic covariance requirement in the study of polarized structure functions within constituent quark models. The investigation clearly shows the relevance of relativistic effects due, in particular to the dynamics of the spin observables in special relativity. In fact two new ingredients play a major rôle in our light-front calculation: i) the presence of high momentum components and ii) the spin dynamics induced by the Melosh transformations.

i) The large amount of high momentum components in the nucleon wave function is generated by the solution of the relativized mass equation (29) and are relevant in reproducing the large x behavior of polarized and unpolarized structure functions. The lack of such high momentum contributions have been repeatedly stressed in connection with non-relativistic calculations [8,30] without reaching a satisfying solution within non-relativistic quark models.

ii) The Melosh rotation dynamics introduce the basic new ingredient in the calculations and its effect is quite sizeable in suppressing the proton response in the region $x \lesssim 0.4$.

The first natural extension of the present discussion is the study of transversity distributions as they will be investigated by Drell-Yan processes. In fact relativity must play a quite sizeable rôle for that observable [31–33] and the light-front dynamics is a privileged tool to study such effects.

In addition to the advantages of our approach we want to stress also its limitations and approximations because a further study should remove them in order to provide a more quantitative study of the nucleon spin within the light-front dynamics.

The most relevant limitation of the present investigation is probably the lack of (non-perturbative) sea contributions at the hadronic scale due to the meson cloud of the nucleon. The effects can be rather large and significant in particular for the spin response of the neutron. Work in this direction is in progress and we want to extend the investigation of non-relativistic approaches [9] inserting the recent successful description of meson cloud

21

[34] within a coherent light-front formulation [35]

A second limitation is determined by the particular choice of the quark-quark interaction of Eq. (29). As mentioned in few points of the present paper the large x behavior of the nucleon response can be affected by the specific choice of the interquark interaction model. Work is in progress to investigate the numerical solutions of more sophisticated hyper-central potentials already discussed in the non-relativistic limit [15]. In addition we did not include hyperfine interaction terms in our analysis and we would like to extend the approach also to the consistent light-front treatment of such interaction.

Finally the factorization scheme dependence is to be investigated in more detail in connection with radiative model studies of the kind discussed in the present paper.

ACKNOWLEDGMENTS

REFERENCES

[1] R.G. Roberts, *The Structure of the Proton*, (Cambridge Univ. Press, Cambridge 19909; T. Muta, *Foundations of Quantum CromoDynamics*, (World Scientific, Singapore 1987).

[2] H.J. Melosh, Phys. Rev. D **9** (1974) 1095.

[3] M. Glück, E. Reya, and A. Vogt, Z. Phys. **C53** (1992) 127; Phys. Lett. **B306** (1993); Z. Phys. **C67** (1995) 433.

[4] for a recent discussion cfr. M. Glück, E. Reya, and A. Vogt, DO-TH 98/07, WUE-ITP-98-019, hep-ph/9806404 Bodo L., E. Reya, MPI-PhT/98-23, DO-TH 98/02, hep-ph/9810270.

[5] G. Parisi and R. Petronzio, Phys. Lett. **B62** (1976) 331.

[6] R.L. Jaffe and G.C. Ross, Phys. Lett. **B93** (1980) 313.

[7] M. Traini, L. Conci and U. Moschella, Nucl. Phys. **A544** (1992) 731; M. Ropele, M. Traini and V. Vento, Nucl. Phys. **A584** (1995) 634. W.Melnitchouk, A.W.Schreiber and A.W.Thomas, Phys. Rev. D **49** (1994) 1183; S. A. Kulagin, W. Melnitchouk, T. Weigl, W. Weise, Nucl.Phys. **A597** (1996) 515; K. Kusaka, G. Piller, A. W. Thomas, A. G. Williams, Phys. Rev. D **55** (1997) 5299; R. Jakob, P. J. Mulders, J. Rodrigues, Nucl. Phys. **A626** (1997) 937; D. I. Diakonov, V. Yu. Petrov, P. V. Pobylitsa, M. V. Polyakov, C. Weiss, Phys. Rev. D **56** (1997) 4069; V. Barone, T. Calarco and A. Drago, Phys. Lett. **B390** (1997) 287; H. Weigel, L. Gamberg, H. Reinhardt, Phys.Rev. D **55** (1997) 6910;

[8] M. Traini, V. Vento, A. Mair and A. Zambarda, Nucl. Phys. **A614** (1997) 472; A. Mair and M. Traini, Nucl. Phys. **A624** (1997) 564;

[9] A. Mair and M. Traini, Nucl. Phys. **A628** (1998) 296.

[10] S. Scopetta, V. Vento and M. Traini, Phys. Lett. **B421** (1998) 64; S. Scopetta, V. Vento

and M. Traini, Phys.Lett. **B442** (1998) 28.

[11] B.D. Keister and W.N. Plolyzou, Adv. in Nucl. Phys. **20** (1991) 225;

[12] E.P. Wigner, Ann Math. **40** (1939) 149.

[13] P.A.M. Dirac, Rev. Mod. Phys. **21**, (1949),392.

[14] F. Coester, Progr. Part. Nucl. Phys. **29** (1992) 1; J. Carbonell, B. Deplanques, V.A. Karmanov and J.-F. Mathiot, Phys. Rep. **300** (1998) 215; S.J. Brodsky, H.C. Pauli and S.S. Pinsky, Phys. Rep. **301** (1998) 299.

[15] M. Ferraris, M.M. Giannini, M. Pizzo, E. Santopinto and L. Tiator, Phys. Lett. **B364** (1995) 231.

[16] F. Coester, K. Dannbom and D.O. Riska, Nucl. Phys. **A634** (1998) 335.

[17] P. Faccioli, thesis, University of Trento 1998, unpublished; M. Traini, P. Faccioli and V. Vento, talk given at the joint Workshop on N⋆ *Physics and non perturbative QCD*, ECT⋆, Trento, May 1998, to be published in the Proceedings.

[18] F. Cardarelli, E. Pace, G. Salmè and S. Simula, Phys. Lett. **B357** (1995) 267; F. Cardarelli, E. Pace, G. Salmè and S. Simula, Phys. Lett. **B371** (1996) 7.

[19] R.D. Ball, S. Forte and G. Ridolfi, Nucl. Phys. **444B** (1995) 287; Phys. Lett. **B378** (1996) 255.

[20] Proceedings of the Workshop *Deep Inelastic Scattering off Polarized Targets: Theory Meets Experiment*, Zeuthen, Germany, September 1-5, 1997.

[21] T. Gehrmann and W.J. Stirling, Phys. Rev. D **53** (1996) 6100.

[22] M. Glück, E. Reya, M. Stratmann and W. Vogelsang, Phys. Rev. D **53** (1996) 4775.

[23] D. de Florian, O.A. Sampayo and R. Sassot, Phys.Rev. D **57** (1998) 5803.

[24] E. Leader, A.V. Sidorov and D.B. Stamenov, Phys. Lett. **B445** (1998) 232; Phys. Rev.

D **58** (1998) 114028; Int. J. Mod. Phys. **A13** (1998) 5573.

[25] R.D. Ball, S. Forte and G. Ridolfi, Phys. Lett. **B378** (1996) 255; G. Altarelli, R.D. Ball, S. Forte and G. Ridolfi, Nucl. Phys. **B496** (1997) 397.

[26] R.L. Jaffe, Phys. Lett. **B365** (1996) 359.

[27] L. Mankiewicz, G. Piller and A. Saalfeld, Phys. Lett. **B395** (1997) 318.

[28] V. Barone, T. Calarco and A. Drago, Phys. Lett. **B431** (1998) 405.

[29] R. Mertig and W.L. van Neerven, Z. Phys. C **70**, (1996) 637; W. Vogelsang, Nucl. Phys. **B475** (1996) 47; T. Weigl and W. Melnitchouk, Nucl. Phys. **B465** (1996) 267.

[30] F.M. Steffens and A.W. Thomas, Nucl. Phys. **A 568** (1994) 798.

[31] R.L. Jaffe and X. Ji, Phys. Rev. Lett. 67 (1991) 552;
Nucl. Phys. B375 (1992) 527.

[32] S. Scopetta and V. Vento, Phys. Lett. **B424** (1998) 25; hep-ph/9707250

[33] F. Cano, P. Faccioli and M. Traini, UTF/99-430, ECT*/01-99, hep-ph/9902345

[34] C. Boros and A.W. Thomas, ADP-99-9/T354; hep-ph/9902472.

[35] F. Cano, P. Faccioli, M. Traini and V. Vento, in preparation.

[36] B. Adeva *et al.* (SMC), Phys. Lett. **B302** (1993) 533. D. Adams *et al.* (SMC), Phys. Lett. **B329** (1994) 399. D. Adams *et al.* (SMC), Phys. Lett. **B357** (1995) 248.

[37] P.L. Anthony *et al.* (E142), Phys. Rev. Lett. **71** (1993) 959. K. Abe *et al.* (E143), Phys. Rev. Lett. **74** (1995) 346. K. Abe *et al.* (E143), Phys. Rev. Lett. **75** (1995) 25.

[38] K. Abe *et al.* (E154), Phys. Rev. Lett. **79** (1997) 26.

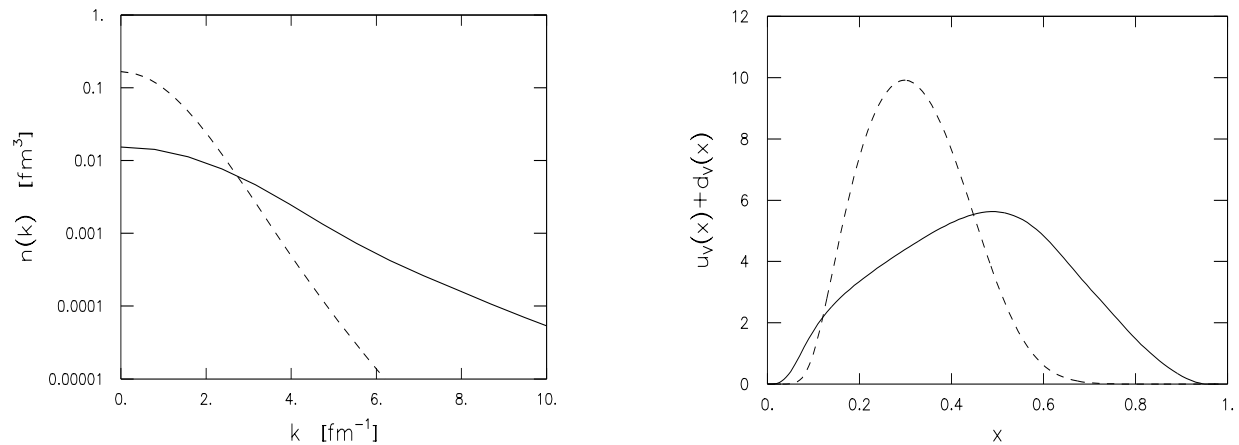[39] CTEQ Collab. H.I. Lai *et al.*, Phys. Rev. D 51 (1995) 4763; Phys. Rev. D 55 (1997) 2862.

FIG. 1. Fig. 1a (left panel): the valence momentum distribution of Eq. (36) as function of $|\mathbf{k}|$. The results of a full covariant light-front calculation (full curve) are compared with the non-relativistic approximation (dashed curve). The corresponding total valence distributions at the hadronic scale are shown on the right panel (Fig. 1b).
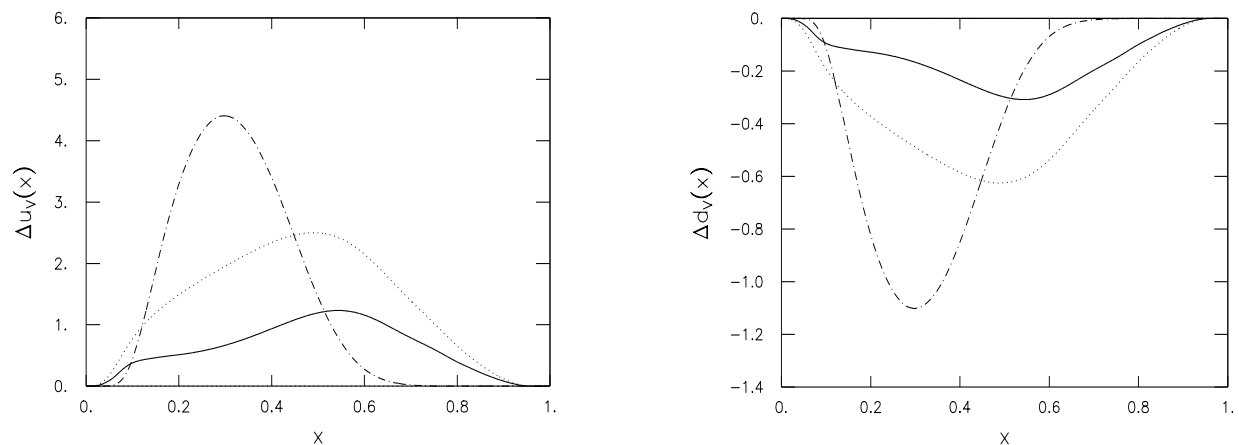

FIG. 2. Left panel (Fig. 2a): the polarized distribution $\Delta u_V(x, \mu_0^2)$ as function of x: the non-relativistic approximation (dot-dashed curve), and the relativized solution of Eq.(29) which neglects Melosh rotations (dotted curve) are compared with the results of a complete light-front calculation (full curve). On the right panel the distibution $\Delta d_V(x, \mu_0^2)$ (same notation).
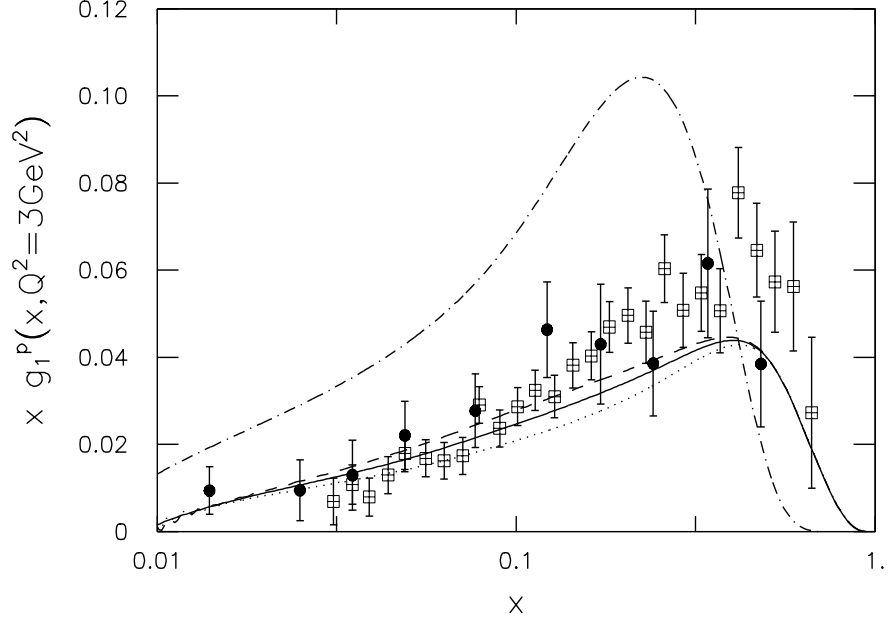
FIG. 3. The proton polarized structure function at $Q^2 = 3$ GeV^2. The full curve represents the NLO ($\overline{MS}$) results of a complete light-front calculation within a scenario where no gluons are present at the hadronic scale (scenario A); the corresponding non-relativistic calculation are shown by the dot-dashed line. Scenario B is summarized by the dotted line in the case of negative polarized gluon fraction ($\int \Delta G = -0.7$ as discussed in the text), and by the dashed line in the case of positive gluon polarization ($\int \Delta G = +0.7$). Data are from SMC [36], and SLAC(E142) [37] experiments.
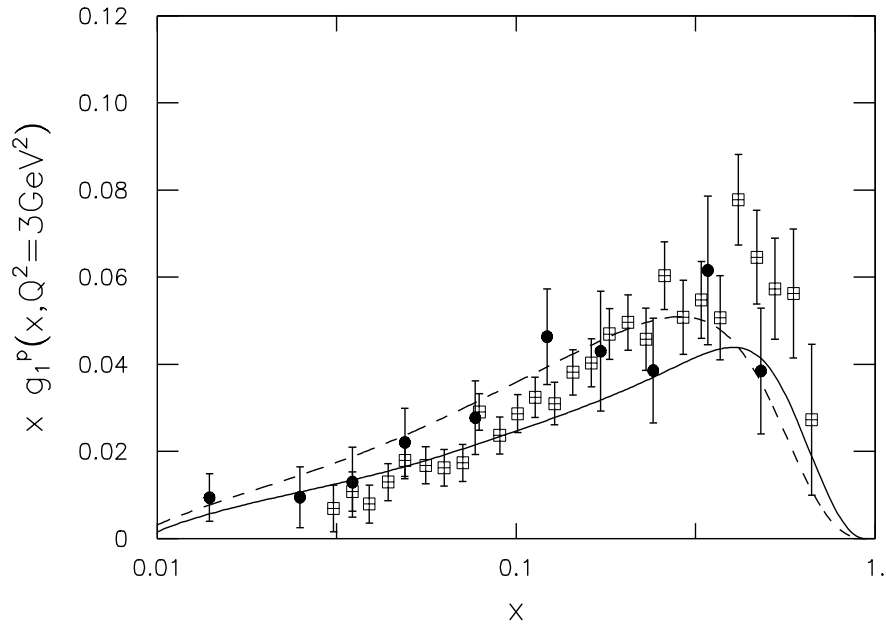
FIG. 4. The proton polarized structure function at $Q^2 = 3$ GeV^2 within scenario A. LO evolution is shown by the dashed curve, the NLO $(\overline{MS})$ results by the full curve. Data as in Fig. 3
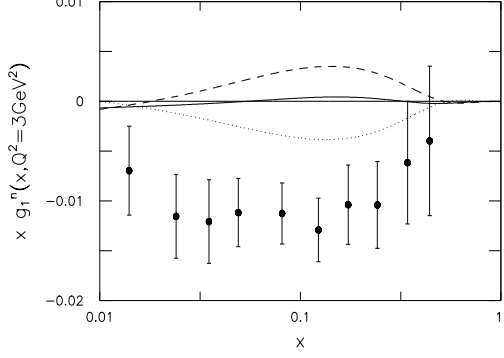
FIG. 5. The NLO ($\overline{MS}$) neutron polarized structure function at $Q^2 = 3\,\text{GeV}^2$ within a complete light-front calculation. The full curve represents the results within a scenario where no gluons are present at the hadronic scale (scenario A). Scenario B is summarized by the dotted line in the case of negative polarized gluon fraction ($\int \Delta G(x, \mu_0^2) = -0.7$ as discussed in the text), and by the dashed line in the case of positive gluon polarization ($\int \Delta G(x, \mu_0^2) = +0.7$). Data are from SLAC(E154) [38] experiments.
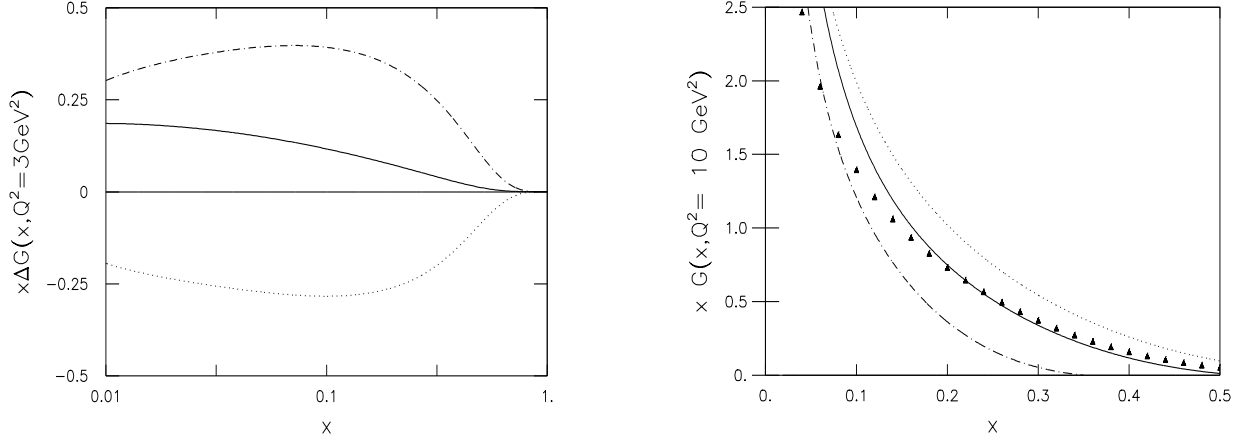
FIG. 6. Left panel: Polarized gluon distributions at $Q^2 = 3\,\text{GeV}^2$ obtained evolving at NLO ($\overline{MS}$) the polarized partons in both scenarios. Scenario A (full line). Scenario B is summarized by the dotted line in the case of negative polarized gluon fraction ($\int \Delta G(x, \mu_0^2) = -0.7$ as discussed in the text), and by the dot-dashed line in the case of positive gluon polarization ($\int \Delta G(x, \mu_0^2) = +0.7$).

Right panel: unpolarized gluon distribution at $Q^2 = 10\,\text{GeV}^2$ obtained evolving at NLO (DIS) unpolarized partons. Scenario A (full line); scenario B (dotted line). For comparison also the results at LO are shown in this case (dot-dashed). CETQ4 NLO (DIS) fit of ref.[39]: full triangles.
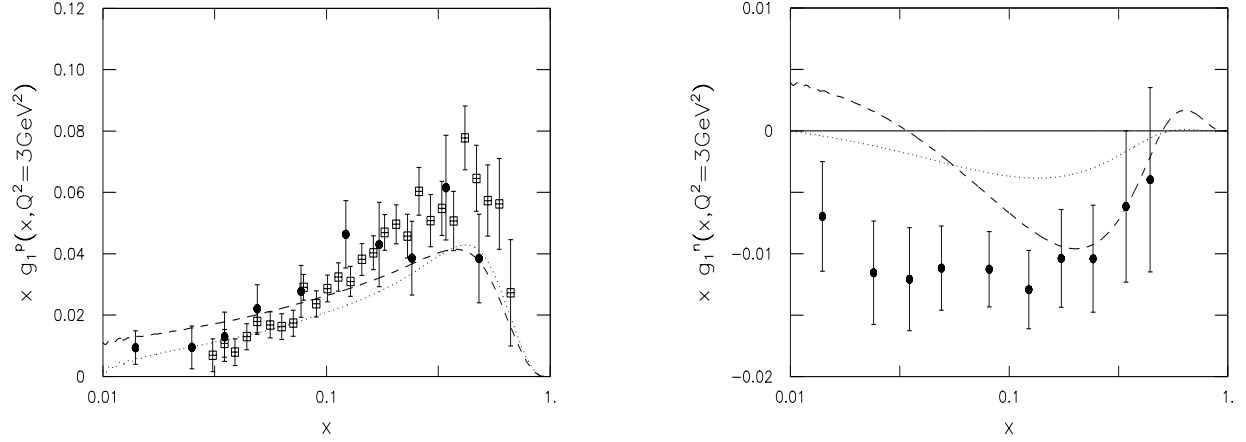
FIG. 7. Scheme dependence of the polarized proton and neutron structure functions at $Q^2 = 3$ GeV^2. $\overline{MS}$ dotted lines; AB: dashed lines.
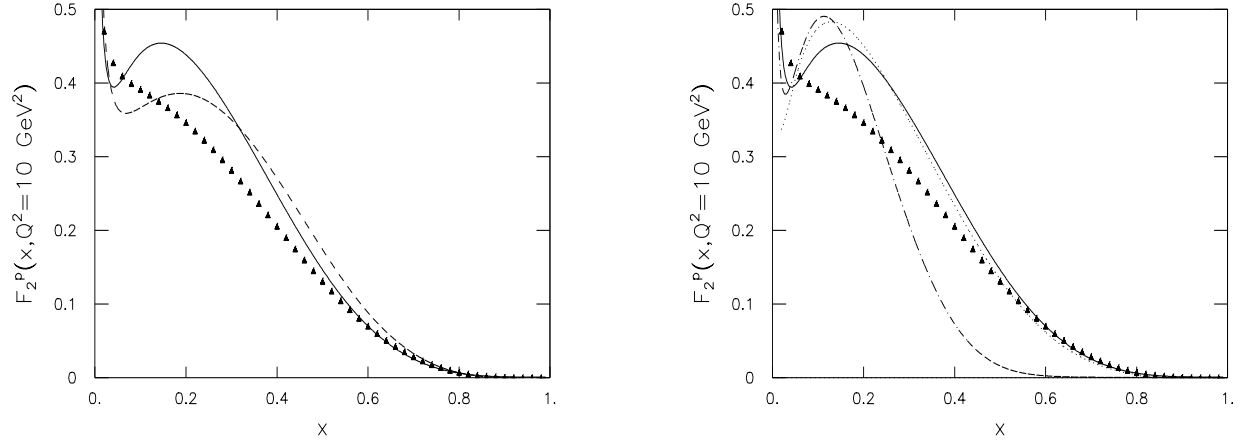

FIG. 8. Left panel: unpolarized F_2 structure function at $Q^2 = 10$ GeV^2 as function of x. LO evolution (dashed) NLO (DIS) full line. Right panel: the F_2 structure function of the proton at $Q^2 = 10$ GeV^2 as predicted by the full light-front calculation at NLO (full curve: scenario A, dotted curve: scenario B) is compared with the non-relativistic approximation (dot-dashed curve). CETQ4 fit of ref.[39]: full triangles.
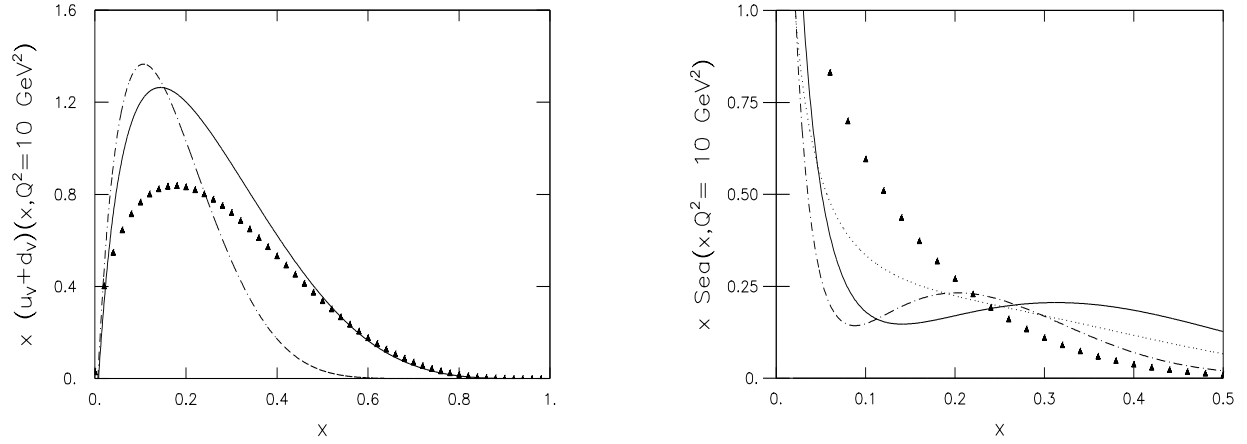
FIG. 9. Left panel: unpolarized NLO (DIS) valence parton distribution at $Q^2 = 10$ GeV^2 as fuction of x. Light-front calculations: full curve; non-relativistic approximation (dot-dashed curve); NLO (DIS) CTEQ4 fit of ref.[39]: full triangles. Right panel: total unpolarized NLO (DIS) sea distribution at at $Q^2 = 10$ GeV^2. Light-front results: scenario A (full curve), scenario B (dotted curve), non-relativistic approximation (dot-dashed curve).